A Small-Signal Stability Index for Power System Dynamic Impact Assessment using Time-domain Simulations

Felix Rafael Segundo Sevilla, *Member, IEEE,* and Luigi Vanfretti, *Member, IEEE,*

***Abstract*—In this paper, a three layer small-signal stability index to assess power system dynamic simulations is presented. The index is calculated from an estimate of the eigenvalues of the system, which are determined using time-series from dynamic simulations. The methodology assumes that no other information about the system (model) is available. In the first layer, which is the main future of the index, a scalar (positive or negative) indicates if any of the modes have a damping ratio less than a pre-defined value. In the second layer, a vector is used to specify which pre-defined damping ratios were violated and finally, in the third layer a matrix is used to retrieve precise information about which mode has violated the pre-defined damping requirements of the system. The proposed index is first illustrated using synthetic data and then the index is validated using simulation data from the KTH-Nordic32 system.**

***Index Terms*—small-signal stability, ringdown, time-domain simulations, severity index**

I. Introduction

THE impact of large-scale power outages in recent years clearly indicates the need for methods that can determine the likelihood of catastrophic system failures.The FP7 iTesla project aims to build a software toolbox to cope with these challenges. Dynamic impact assessment of detailed time-domain simulations is part of the off-line analysis workflow within the iTesla toolbox[1]. The aim is to develop offline criteria to support online analysis functions.

After performing a dynamic simulation for a specific contingency, an appropriate post-contingency severity index needs to be determined in order to classify the impact of the contingency. To do so, a set of scalars, vectors and matrices define the stability index that provides a measure of how severe the contingency is. The main advantage of this index is its simplicity to classify a given contingency using the different layers. The index has been designed with the requirement of fast computation and to provide a good measure of how severe the contingency is. These requirements differentiate the small-signal stability index presented here to those described in [1], [2] and [3].

This work was supported in part by the EU-funded FP7 iTesla project and by Statnett SF, the Norwegian Transmission System Operator.

F. R. Segundo Sevilla and L. Vanfretti are with the Electric Power Systems Department at KTH Royal Institute of Technology in Stockholm, Sweden (e-mail: *frss@kth.se* and *luigiv@kth.se*).

L. Vanfretti is with Statnett SF, Research & Development, Oslo, Norway (e-mail: *luigi.vanfretti@statnett.no*).

[1]iTESLA(Innovative Tools for Electrical System Security within Large Areas), online: www.itesla-project.eu

The reminder of this paper is organized as follows. Section II presents the methodology and each of the stages required to calculate the small-signal stability index. Section III explains how to interpret the results by describing the three different layers. In Section IV, a simple example (using synthetic data) is given to illustrate the application and interpretation of the index. Later, in Section V, the application of the index is demonstrated and validated through nonlinear simulations using the KTH-NORDIC32 system. Finally, Section VI summarizes the results and outlines future work.

II. Small-Signal Stability Index

Small-signal stability refers to the ability of a power system to maintain synchronism under small disturbances. Instability may arise in two forms: a) increase of rotor angle due to lack of sufficient synchronization torque, or b) rotor oscillations of increasing amplitude due to lack of sufficient damping torque [4]. In this section, the different stages required to calculate the small-signal index are defined.

A. Pre-precessing input signals

Dynamic simulations provide time-series with useful information to assess the dynamic performance of the system (e.g. active power flows on critical lines). To estimate the eigenvalues of the system, the first step is to choose signals with the highest oscillation content. This can be performed by calculating the energy of each signal and sorting them in descending order. First, signals $y(t)$ are detrended to remove linear trends and put all of them in the same reference, and then the energy of the time varying signals can be calculated as in (1).

$$\hat{y}(t) = y(t) - y_{mean}(t), \qquad E(t) = \int_{-\infty}^{\infty} |\hat{y}(t)|^2 \, dt \tag{1}$$

where $y(t) \in \Re^p$ are the signals to be analyzed and p is the total number of signals, $y_{mean}(t) \in \Re^p$ are the mean values, $\hat{y}(t) \in \Re^p$ are the detrended signals and $E(t) \in \Re^p$ are the energy of all signals.

B. Frequency Screening

Because dynamic simulations provide a large number of signals to be analyzed, it is useful to divide the signals into a smaller subgroup to facilitate calculations. Signals can be

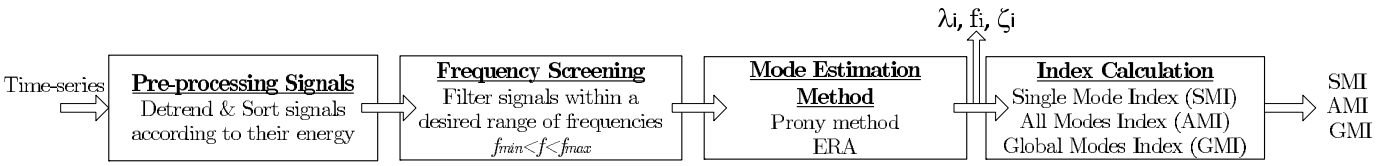

Fig. 1. Flow chart of the index calculation procedure.

classified according to their frequency, so only signals within a desired frequency range are analyzed, e.g. between 0.1 and 1 Hz for inter-area modes. The classification can be carried out using the Fast Fourier Transform (FFT) as described below

$$Y(k) = \sum_{n=0}^{N-1} y(n) e^{-i2\pi k \frac{n}{N}}, \qquad k = 0, \ldots, N-1. \tag{2}$$

N is the size of $y(t)$. $Y(k)$ is a vector of complex numbers, the largest magnitudes of the complex vector $|Y(k)|$ are the frequencies of the signal $y(t)$.

C. Mode Estimation Methods

The mode estimation problem may be posed as follows: given a set of measurements that vary with time, it is desired to fit a time-varying waveform of pre-specified form (such as (4)) to the actual waveform. Consider the following linear system

$$\dot{x}(t) = Ax(t) + Bu(t), \quad y(t) = Cx(t) \tag{3}$$

where $x(t) \in \Re^n$ is the state of the system, $u(t) \in \Re^q$ is the control input and $y(t) \in \Re^p$ are the outputs of the system. A, B and C matrices are constant and of appropriate dimensions. Each individual element $x_i(t)$ is given by:

$$x_i(t) = \sum_{i=1}^{n} r_i x_i(0) e^{\lambda_i t} = \sum_{i=1}^{n} a_i e^{\sigma_i t} \cos(\omega_i t + \theta_i) \tag{4}$$

where the parameter r_i is the residue of the mode i, $x_i(0)$ is derived from initial conditions, and λ_i represents the eigenvalues of A, the frequency f and damping ratio ζ of mode λ_i are given as follows

$$\lambda_i = \sigma_i + j\omega_i, \qquad f_i = \frac{\omega_i}{2\pi}, \qquad \zeta_i = \frac{-\sigma_i}{\sqrt{\sigma_i^2 + \omega_i^2}} \tag{5}$$

The main target in modal identification is to determine the eigenvalues of system (3). For full details about linear ring-down analysis methods such as: Prony's method, Eigenvalue Realization Algorithm (ERA), Matrix pencil and nonlinear methods, see [5].

D. Index Calculation

After estimating the modes from time-series, it is possible to calculate the distance from each mode to a pre-defined damping ratio to evaluate the stability condition of the system. Typically, a damping ratio below 5% is unacceptable in power systems because following a disturbance, oscillations in the signals will last for several seconds thereby affecting the system's dynamic performance. In the worst case (having negative damping), increasing oscillations will appear indicating

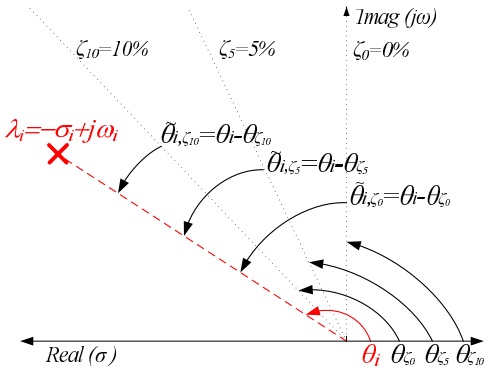

Fig. 2. Distance $\tilde{\theta}$ (in radians) from the ith mode (λ_i) to different pre-defined damping ratios $\zeta_0 = 0\%$, $\zeta_5 = 5\%$ and $\zeta_{10} = 10\%$, respectively.

that the system is unstable. A summary of the procedures required to apply the small-signal stability index to time-series is described in Figure 1. More details about the index are described in the following section.

III. Three-Layer Small-Signal Stability Index

In this section the small-signal stability index is explained. The index has three layers, it provides a measure related to the stability of the system and is based on the damping ratio of the estimated system modes. The measure is the angular distance (in radians) from each mode to a pre-defined damping ratio, as seen in Figure 2. The three layers of the index are:

- Single Mode Index (SMI), a matrix.
- All Modes Index (AMI), a vector.
- Global Modes Index (GMI), a scalar.

The **SMI** offers the most detailed source of information, but for a system with multiple modes, it is not easy to interpret. The matrix of data is described as follows

$$SMI = \begin{bmatrix} \tilde{\theta}_{1,\zeta_0} & \tilde{\theta}_{1,\zeta_5} & \tilde{\theta}_{1,\zeta_{10}} & \cdots & \tilde{\theta}_{1,\zeta_j} \\ \vdots & \vdots & \vdots & \ddots & \vdots \\ \tilde{\theta}_{i,\zeta_0} & \tilde{\theta}_{i,\zeta_5} & \tilde{\theta}_{i,\zeta_{10}} & \cdots & \tilde{\theta}_{i,\zeta_j} \end{bmatrix} \tag{6}$$

and

$$\begin{aligned} \tilde{\theta}_{i,\zeta_j} &= \theta_i - \theta_{\zeta_j} \\ \theta_i &= cos^{-1}(\zeta_i) \\ \theta_{\zeta_j} &= \pi - cos^{-1}(\zeta_j) \end{aligned} \tag{7}$$

where $\tilde{\theta}_{i,\zeta_j}$ is the (i,j) element of SMI, ζ_i and θ_i are the damping ratio and angle of the ith mode λ_i, respectively. ζ_j and θ_{ζ_j} are the jth pre-defined damping ratios and angles, respectively.

SMI provides the individual distance of each mode to a pre-defined damping ratio, e.g. $\zeta_0 = 0\%$, $\zeta_5 = 5\%$ and $\zeta_{10} = 10\%$. If any of the elements of SMI is negative, this indicates that

the mode corresponding to the specific row, has a damping ratio less than the required for that column. For instance, lets assume that element (2,2) in (6) is negative ($\tilde{\theta}_{2,\zeta_5} < 0$), then mode λ_2 has a damping ratio less than 5% ($\zeta_2 < 5\%$) and consequently element (2,3) in (6) is also negative; this mode is violating the damping ratios ζ_5 and ζ_{10}, respectively.

AMI facilitates the interpretation of SMI, it is a vector and it gives the minimum distance of the modes with respect to each of the pre-defined damping ratios ζ_j as described below

$$AMI=\left[\,\hat{\theta}_{\zeta_0} \quad \hat{\theta}_{\zeta_5} \quad \hat{\theta}_{\zeta_{10}} \quad \cdots \quad \hat{\theta}_{\zeta_j}\,\right], \quad \hat{\theta}_{\zeta_j} = _{min}\, |\tilde{\theta}_{i,\zeta_j}| \quad (8)$$

If one value of AMI is negative, this means that at least one mode has a damping ratio less than the one required.

GMI gives a global interpretation of the modes respect to all pre-defined damping ratios, is the minimum distance among all modes respect to all pre-defined ratios and is described below

$$GMI = \Theta_{\zeta_j}, \qquad \Theta_{\zeta_j} = _{min}\, |\hat{\theta}_{\zeta_j}| \cdot \quad (9)$$

Remark: If the system has a single mode, then SMI and AMI are the same. If the system is unstable, all the elements in SMI, AMI and GMI will be negative for the corresponding mode.

IV. Illustrative Example

In this section an example to illustrate the interpretation of the SMI, AMI and GMI indexes is presented, and their ability to identify signals with multiple modes is demonstrated. Two synthetic signals $y_1(t)$ and $y_2(t)$ of known frequency and damping were generated using (10)

$$\begin{aligned} c_i(t) &= 1 - e^{-\left(\zeta_i - \sqrt{\zeta_i^2-1}\omega_i t\right)}, \quad i = 1,2,3 \\ d_j(t) &= 1 - e^{-\left(\zeta_j - \sqrt{\zeta_j^2-1}\omega_i t\right)}, \quad j = 1,2,3 \\ y_1(t) &= c_1(t) * c_2(t) * c_3(t) \\ y_2(t) &= d_1(t) * d_2(t) * d_3(t) \end{aligned} \quad (10)$$

Figures 3 (a)-(c) depict each stage of the application of the small-signal index described in Section II. The time-series of signals $y_1(t)$ and $y_2(t)$ are described in Figure 3 (a). First, the input signals were detrended and sorted according to their energy, then a frequency screening is applied to identify the frequencies within a range of interest as shown in Figure 3 (b). Next,linear ringdown analysis method was applied using Prony in Figure 3 (c), and in the last step, six different modes were estimated as shown in Figure 3 (d) and Table I.

TABLE I
IDENTIFIED MODES WITHIN THE FREQUENCY RANGE OF: 0.10 AND 1.0 HZ

Mode	$\sigma + j\omega$	f (Hz)	ζ (%)
λ_1	-0.0980 + j 0.7476	0.1190	13.0
λ_2	-0.0867 + j 1.4425	0.2296	6.0
λ_3	-0.0905 + j 3.0146	0.4798	3.0
λ_4	-0.0653 + j 3.2666	0.5199	2.0
λ_5	-0.0540 + j 5.4033	0.8600	1.0
λ_6	-0.4675 + j 5.8246	0.9270	8.0

The SMI, AMI and GMI indexes are summarized in Table II. The value of the GMI is negative: at least one mode has violated one of the pre-defined damping ratios. For multiple scenarios, GMI provides sufficient information to classify each case study using a binary decision. A review of AMI, illustrates that elements $(1,2)$ and $(1,3)$ are negative, showing that at least one mode has violated the pre-defined damping ratios ζ_{10} and ζ_5 set to 10% and 5%, respectively. AMI can be used as a threshold to classify case studies where a minimum damping is required. After examining SMI it is possible to conclude that modes λ_3, λ_4 and λ_5 are violating the damping ratio ζ_5, and modes λ_2 to λ_5 are violating the damping ratio ζ_{10}; as indicated by their negative numbers highlighted in bold in Table II. Figure 3 (d) confirms the indexes results. SMI retrieves detailed stability information about each mode.

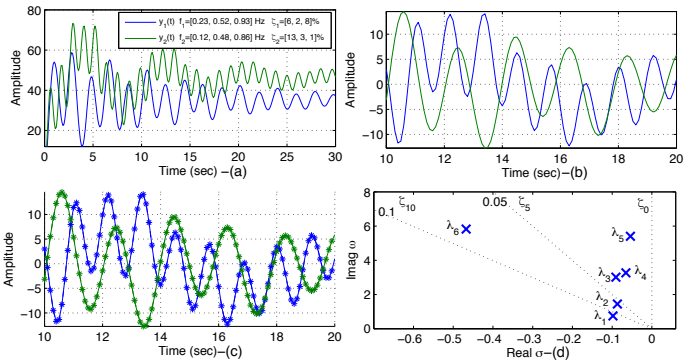

Fig. 3. (a) Analyzed time-series, (b) Detrended and selected data, (c) Signal estimation from ringdown analysis, (d) Estimated Modes.

TABLE II
SMALL-SIGNAL STABILITY INDEXES FOR THE SYNTHETIC CASE

	Θ_{ζ_j}
GMI	**-0.0902**

	$\hat{\theta}_{\zeta_0}$	$\hat{\theta}_{\zeta_5}$	$\hat{\theta}_{\zeta_{10}}$
AMI	0.0100	**-0.0400**	**-0.0902**

SMI	$\tilde{\theta}_{i,\zeta_0}$	$\tilde{\theta}_{i,\zeta_5}$	$\tilde{\theta}_{i,\zeta_{10}}$
λ_1	0.1304	0.0803	0.0302
λ_2	0.0600	0.0100	**-0.0401**
λ_3	0.0300	**-0.0200**	**-0.0702**
λ_4	0.0200	**-0.0300**	**-0.0802**
λ_5	0.0100	**-0.0400**	**-0.0902**
λ_6	0.0801	0.0301	**-0.0201**

V. Application using a power system model

A. Power System Description

The KTH-Nordic32 system was constructed from the data proposed in [6], further details are available in [7]. The one-line diagram is shown in Figure 4 and it is comprised of 52 buses, 80 transmission lines and 20 generators. There are 12 hydro generators located in the North and equivalent areas, the rest are thermal generators located in the Central and South areas. This weakly coupled system exhibits lightly damped low frequency inter-area oscillations. The two lowest damping modes have a frequency of 0.46 Hz and 0.78 Hz, respectively and a damping ratio of 4.08% and 4.98%, respectively. Although mode shapes are not shown here, λ_1 is related to the swing of the North and Equivalent machines against the

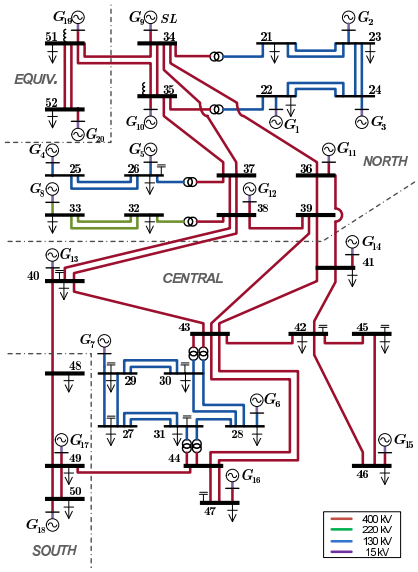

Fig. 4. The KTH-Nordic32 power system.

Central and South machines, while λ_2 is related to the swing of the Central machines against the Equivalent and South machines. Both modes have a low damping ratio.

B. Case study 1: Single Contingency Analysis

A 3-phase fault of 160 msec was applied at bus 40. After the disturbance, the proposed indexes SMI, AMI and GMI, where computed from time-series of the active power flow on different lines. Two modes were identified and are shown in Table III, note that the real part of λ_1 is positive and has a negative damping ratio (-7.05%) indicating an unstable condition in the system.

B.1 Analysis of the Index Calculation

Figure 5 depicts the different stages of the indexes calculation. Figure 5 (a) shows the effects of the disturbance in the active power flow of the 80 transmission lines, while Figure 5 (b) presents the post-disturbance time-series. The application of the ringdown method (Prony) and identification results are shown in Figure 5 (c). The location of the modes in the complex plain is shown in Figure 5 (d). Table IV presents the value of the small-signal indexes from where it is possible to conclude that λ_1 is unstable, as indicated by the negative numbers of elements $(1,1)$, $(1,2)$ and $(1,3)$ of SMI and the negative damping ratio in Table IV. λ_2 has damping ratio above 5% as indicated by the positive distances $(2,1)$ and $(2,2)$ in elements of SMI.

In this case the disturbance destabilizes λ_1 and does not provide enough excitation to λ_2 and thus, the time-domain simulation does not show much activity in the time-series to obtain a better estimation. The important aspect to keep in mind here is that the mode which is most affected by the contingency instability is detected by the indexes, and that leads to the system's instability.

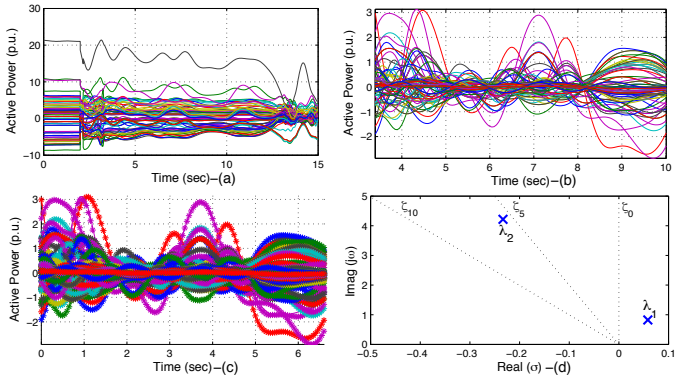

Fig. 5. (a) Analyzed time-series, (b) Detrended and selected data, (c) Signal estimation from ringdown analysis, (d) Estimated Modes.

TABLE III
ESTIMATED MODES, FREQUENCIES AND DAMPING (CASE STUDY 1)

Mode	$\sigma + j\omega$	f (Hz)	ζ (%)
λ_1	0.0583 + j 0.8240	0.1311	-7.0588
λ_2	-0.2333 + j 4.2171	0.6712	5.5249

TABLE IV
SMALL-SIGNAL STABILITY INDEXES FOR THE NORDIC SYSTEM (CASE STUDY 1)

	Θ_{ζ_j}
GMI	**-0.0706**

	$\hat{\theta}_{\zeta_0}$	$\hat{\theta}_{\zeta_5}$	$\hat{\theta}_{\zeta_{10}}$
AMI	**-0.0706**	**-0.1207**	**-0.1708**

SMI	$\tilde{\theta}_{i,\zeta_0}$	$\tilde{\theta}_{i,\zeta_5}$	$\tilde{\theta}_{i,\zeta_{10}}$
λ_1	**-0.0706**	**-0.1207**	**-0.1708**
λ_2	0.0553	0.0053	**-0.0449**

C. Case study 2: Multiple Contingency Analysis

In this case multiple contingencies were analyzed, the simulations consider 3-phase faults applied to different buses for a fixed duration of 100 msec (Case 2.A) and for a random duration between 20 and 150 msec (Case 2.B). Active power flows were used as input signals.

C.1 Case 2.A: Fixed Fault Duration

A 3-phase fault of 100 msec was applied at each of the 32 buses of the system (32 simulations). The median values of the identified modes are shown in Table V, where the standard deviation is also included. Figure 6 (a) depicts the location in the complex plain of the modes (λ_1 in red and λ_2 in blue) and the location of the median values in black. From these results, it can be seen how λ_1 is better estimated than λ_2. The standard deviation is lower for λ_1 and the poles location are closer to each other as shown by the blue crosses in Figure 6 (a), λ_1 is more visible than λ_2, this can be justified in a similar way as in the example in Section V-B. The median values of SMI, AMI and GMI are shown in Table VI, it is possible to conclude that λ_1 has a damping ratio below 5% as indicated by the negative numbers in SMI and that λ_2 has a damping ratio less than 10% as indicated by the negative number in the element $(2,3)$ of SMI. Figure 7 shows the fitted normal distribution of the frequency and damping ratio for both modes after the disturbances in the system.

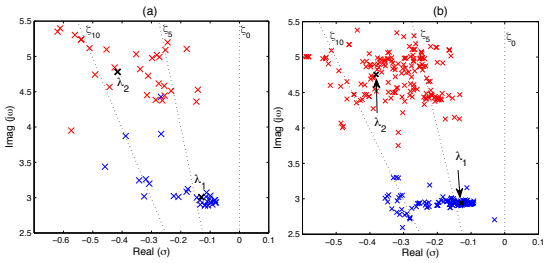

Fig. 6. Estimated modes λ_1 in red and λ_2 in blue and median values in black for both: (a) Case study 2.A and (b) Case study 2.B

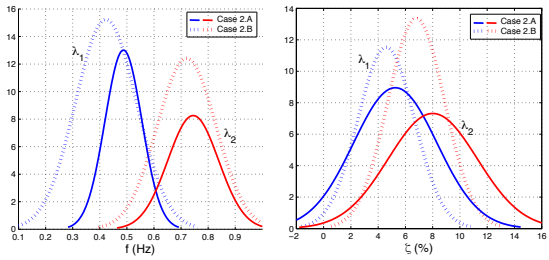

Fig. 7. Fitted normal distribution of the estimated frequencies and damping ratios for both modes λ_1 in blue and λ_2 in red and both case studies

TABLE V
MEDIAN OF THE ESTIMATED MODES, FREQUENCIES AND DAMPING (CASE STUDY 2.A)

Mode	$\sigma + j\omega$	f (Hz)	ζ (%)	*std*
λ_1	-0.1298 + j 3.0069	0.4763	4.56	0.0681
λ_2	-0.4153 + j 4.7811	0.7609	6.99	0.1006

TABLE VI
SMALL-SIGNAL STABILITY INDEXES FOR THE NORDIC SYSTEM - MEDIAN VALUES (CASE STUDY 2.A)

	Θ_{ζ_j}
GMI	**-0.0545**

	$\hat{\theta}_{\zeta_0}$	$\hat{\theta}_{\zeta_5}$	$\hat{\theta}_{\zeta_{10}}$
AMI	0.0456	**-0.0044**	**-0.0545**

SMI	$\tilde{\theta}_{i,\zeta_0}$	$\tilde{\theta}_{i,\zeta_5}$	$\tilde{\theta}_{i,\zeta_{10}}$
λ_1	0.0456	**-0.0044**	**-0.0545**
λ_2	0.0700	0.0199	**-0.0302**

C.2 Case 2.B: Random Fault Duration

Five 3-phase faults of random duration between 120 and 250 msec were applied at each of the 32 buses (160 simulations). The identified modes are plotted in Figure 6 (b), the fitted normal distribution of the frequency and damping ratio for both modes are shown in Figure 7 (dotted curves) and the median values are shown in Table VII. Note that the standard deviation values for both modes are smaller than in the previous case study. Table VIII shows the SMI, AMI and GMI index for this study case.

C.3 Comparison of Case 2.A and Case 2.B

Analyzing results from case studies 2.A and 2.B, is possible to observe that incrementing the severity of the disturbances in the network improves the identification of the system modes as indicated by the reduction of the standard deviation on Table V and VII. Larger disturbances excite relevant modes facilitating its identification. Altough, λ_1 is the most visible mode in the system as indicated by the concentration of blue crosses in Figures 6 (a) and (b), λ_2 can be identified applying the correct disturbance.

TABLE VII
MEDIAN OF THE ESTIMATED MODES, FREQUENCIES AND DAMPING (CASE STUDY 2.B)

Mode	$\sigma + j\omega$	f (Hz)	ζ (%)	*std*
λ_1	-0.1282 + j 2.9392	0.4698	3.98	0.0054
λ_2	-0.3818 + j 4.7539	0.7566	5.94	0.0938

TABLE VIII
SMALL-SIGNAL STABILITY INDEXES FOR THE NORDIC SYSTEM - MEDIAN VALUES (CASE STUDY 2.B)

	Θ_{ζ_j}
GMI	**-0.0652**

	$\hat{\theta}_{\zeta_0}$	$\hat{\theta}_{\zeta_5}$	$\hat{\theta}_{\zeta_{10}}$
AMI	0.0349	**-0.0151**	**-0.0652**

SMI	$\tilde{\theta}_{i,\zeta_0}$	$\tilde{\theta}_{i,\zeta_5}$	$\tilde{\theta}_{i,\zeta_{10}}$
λ_1	0.0349	**-0.0151**	**-0.0652**
λ_2	0.0595	0.0095	**-0.0406**

VI. CONCLUSIONS

In this paper a three layer severity index to assess the power system small-signal stability problem has been described. The index is calculated using time-series (active power flows) from dynamic simulations without any information about the mathematical model of the system. The index is comprised by a matrix (SMI), a vector (AMI) and a scalar (GMI) to facilitate interpretation. Active and reactive power trough transmission lines were utilized as inputs to calculate the index. Altough Prony's procedure was used as ringdown method, the index is not limited to this approach and can use any other linear or non-linear methodology. Nonlinear simulations using the KTH-Nordic32 power system model were performed to validate the procedure. Future work will focus to the application of this index to time-series obtained from synchronized phasor measurements in both off-line and near real-time analysis.

REFERENCES

[1] X. Xie, S. Zhang, J. Xiao, J. Wu, and Y. Pu, "Small signal stability assessment with online eigenvalue identification based on wide-area measurement system," in *Transmission and Distribution Conference and Exhibition: Asia and Pacific, 2005 IEEE/PES*, 2005, pp. 1–5.

[2] U. Kerin, T. Tuan, E. Lerch, and G. Bizjak, "Small signal security index for contingency classification in dynamic security assessment," in *IEEE Trondheim PowerTech*, 2011, pp. 1–6.

[3] J. Rueda, D. Colome, and I. Erlich, "Assessment and enhancement of small signal stability considering uncertainties," *IEEE Transactions on Power Systems*, vol. 24, no. 1, pp. 198–207, 2009.

[4] G. Rogers, Ed., *Power System Oscillations*. Springer, 1999.

[5] J. Sanchez-Gasca, "Identification of electromechanical modes in power systems," *IEEE Task Force on Identification of Electromechanical Modes*, June 2012.

[6] T. Vancustem, "Description, modeling and simulation results of a test system for voltage stability analysis," *Technical Report Version 5, IEEE Working Group on Test Systems for Voltage Stability Analysis*, July 2013.

[7] Y. Chompoobutrgool, W. Li, and L. Vanfretti, "Development and implementation of a nordic grid model for power system small-signal and transient stability studies in a free and open source software," in *IEEE Power and Energy Society General Meeting,*, 2012, pp. 1–8.